

Development of Two Rhenium-Containing Superalloys for Single-Crystal Blade and Directionally Solidified Vane Applications in Advanced Turbine Engines

K. Harris, G.L. Erickson, S.L. Sikkenga, W.D. Brentnall, J.M. Aurrecoechea, and K.G. Kubarych

A team approach involving several turbine engine companies using the concepts of simultaneous engineering has been used to successfully develop CMSX-4[®] alloy for turbine blade applications. CMSX-4 alloy is a second-generation, single-crystal cast nickel-base superalloy containing 3% Re and approximately 70% volume fraction of γ' . The high level of balanced properties determined by laboratory evaluation has been confirmed during field testing of the Solar[®] Mars T-14000 industrial gas turbine with CMSX-4 single-crystal (SX) blades in both the coated and bare condition. A similar collaborative approach has resulted in the successful development of CM 186 LC[®] alloy for complex, directionally solidified (DS) columnar grain vane segments. CM 186 LC alloy is a second-generation DS columnar grain cast nickel-base superalloy containing 3% Re and approximately 65% volume fraction of γ' . Excellent component producibility and quality is demonstrated. Turbine engine testing is scheduled to commence by the end of 1993.

Keywords

cast superalloys, directionally solidified columnar grain, rhenium, single-crystal blade

1. Introduction

INCREASED operating temperatures and higher rotational speeds, resulting in increased component stresses, are primary goals in the continuing development of the gas turbine to provide improved fuel efficiency and power-to-weight performance. Cost reduction from improvements in turbine component producibility and process yield, and through gains in airfoil component durability, is an additional objective.

The greatest advances in metal temperature and stress capability for turbine blades in the last 30 years has been the result of the development of single-crystal superalloy, casting process and engine application technology pioneered by Pratt and Whitney Aircraft.^[1-19] The compositions of the first-generation single-crystal superalloys that have attained turbine engine application status are shown in Table 1.* These alloys are characterized by similar creep-rupture strengths. However, they exhibit differing single crystal castability, residual γ/γ' eutectic phase content following solutioning, propensity for recrystallization during solution heat treatment, absence or presence of carbides, impact and mechanical high- and low-cycle fatigue properties (HCF and LCF), environmental oxidation, and hot corrosion properties and density.

* CMSX-2[®], CMSX-3[®], CMSX-4[®], CMSX-6[®], CM 247 LC[®], and CM 186 LC[®] are registered trademarks of the Cannon-Muskegon Corporation. [SPS Technologies]

K. Harris, G.L. Erickson, and S.L. Sikkenga, Cannon-Muskegon Corporation, Muskegon, Michigan 49443 USA; SPS Technologies; and W.D. Brentnall, J.M. Aurrecoechea, and K.G. Kubarych, Solar[®] Turbines, Inc., San Diego, California 92186 USA; [Caterpillar[®]]

Carbon has been included in some single-crystal alloy compositions to assist vacuum induction refining and alloy cleanliness. However, the carbide interfaces with the metal matrix are surfaces of high energy and can act as crack initiation sites along with fractured carbides during creep deformation and mechanical fatigue loading.^[20] Casting micropores in non-hot isostatically pressed (HIPed) single-crystal castings can also be important in determining mechanical fatigue life. Fatigue cracking initiates at the micropores, and crack initiation can occur quite early in notched specimens. It is reported that the micropores in a single-crystal first-generation alloy become coated with γ' during high-temperature service exposure, and fatigue cracks nucleate in the γ' , coating the pore.^[21]

Turbine engine experience with the first-generation single-crystal alloys has resulted in process developments being combined with second-generation alloy development to improve and maximize overall properties of the turbine airfoil components.^[23] Microstructures can be optimized to be fully solutioned and HIPed, to contain neither γ/γ' eutectic phase nor regions of incipient melting, carbides, or microporosity.^[22] The published compositions of several second-generation single-crystal alloys are shown in Table 2.

The Allison Gas Turbine Division of GMC has reported completion of initial turbine engine testing of a highly advanced variable-cycle core that offers the potential for doubling powerplant hot section life and reducing high-pressure turbine weight by 30%.^[25] Eventually, this integrated high performance turbine engine technology (IHPTET) engine is targeted to double engine thrust-to-weight ratio from the best current (10:1) to 20:1, while cutting fuel consumption by 38%. The engine features a turbine wheel with blades fabricated from Lamilloy[®] single-crystal materials.**

CMSX-4 alloy is a second-generation single-crystal superalloy containing 3% Re. It has been developed to maximize

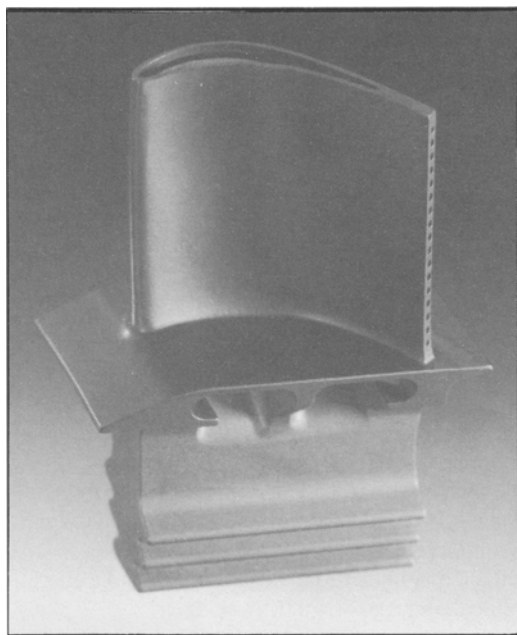
** Lamilloy[®] is a registered trademark of Allison Gas Turbine Division (GMC), Indianapolis, Indiana, USA.

Table 1 First-generation single-crystal superalloys

Alloy	Nominal composition, wt%										Density, kg/dm ³	
	Cr	Co	Mo	W	Ta	V	Nb	Al	Ti	Hf		Ni
PWA 1480 ^[11]	10	5	...	4	12	5.0	1.5	...	bal	8.70
René N-4 ^[2,3]	9	8	2	6	4	...	0.5	3.7	4.2	...	bal	8.56
SRR 99 ^[5,6]	8	5	...	10	3	5.5	2.2	...	bal	8.56
RR 2000 ^[5,6]	10	15	3	1	...	5.5	4.0	...	bal	7.87
AM1 ^[8]	8	6	2	6	9	5.2	1.2	...	bal	8.59
AM3 ^[19]	8	6	2	5	4	6.0	2.0	...	bal	8.25
CMSX-2 ^[11,14]	8	5	0.6	8	6	5.6	1.0	...	bal	8.56
CMSX-3 ^[11,14]	8	5	0.6	8	6	5.6	1.0	0.1	bal	8.56
CMSX-6 ^[15]	10	5	3	...	2	4.8	4.7	0.1	bal	7.98
AF 56 ^[7]	12	8	2	4	5	3.4	4.2	...	bal	8.25

Table 2 Second-generation single-crystal alloys

Alloy	Nominal composition, wt%										Density, kg/dm ³
	Cr	Co	Mo	W	Ta	Re	Al	Ti	Hf	Ni	
CMSX-4 ^[23]	6.5	9	0.6	6	6.5	3	5.6	1.0	0.1	bal	8.70
PWA 1484 ^[17]	5	10	2	6	9	3	5.6	...	0.1	bal	8.95
SC 180 ^[36]	5	10	2	5	8.5	3	5.2	1.0	0.1	bal	8.84
MC2 ^[24]	8	5	2	8	6	...	5.0	1.5	...	bal	8.63

**Fig. 1** Solar Mars T-14000 single-crystal first-generation blade CMSX-4 alloy.

overall properties, through collaborative programs with several turbine engine companies, involving close to one hundred 400-lb (182-kg) heats and seven 8000-lb (3630-kg) production size heats. The aim chemistry of the alloy and its heat treatment (including the HIP option) have been developed to optimize microstructure and effect low levels of residual microsegregation.

Complex, cooled, thin-wall vane segments, often with large overhanging integral shrouds and wide chord three-dimensional computer-designed airfoils, can be difficult and expensive to manufacture as single crystals due to grain problems and

recrystallization occurring during solution heat treatment resulting from residual casting stresses. CM 186 LC alloy, a second-generation DS columnar grain superalloy containing 3% Re, has been developed with turbine engine company collaboration, with both component producibility and economic objectives in mind.

1.1 CMSX-4 Superalloy

1.1.1 Chemistry

CMSX-4 alloy, developed using a multi-dimensional approach^[23] over a 10-year period, achieves a high level of balanced properties. The alloy is derived from CMSX-2[®] alloy^[11,14] and draws the beneficial strengthening effects of rhenium. The nominal composition and density are shown in Table 2.

It is known that rhenium partitions mainly to the γ' matrix, retards coarsening of the γ' strengthening phase, and increases the γ/γ' misfit.^[26] Atom probe microanalyses of rhenium-containing modifications of PWA 1480 and CMSX-2 alloys reveal the occurrence of short-range order in the γ matrix.^[27,29] Small rhenium clusters (approximately 1.0 nm in size) are detected in the alloys. The rhenium clusters act as efficient obstacles against dislocation movement in the γ matrix compared to isolated solute atoms in solid solution and thereby play a significant role in improving alloy strength. Some studies have shown that approximately 20% of the rhenium in this type of alloy partitions to the γ' ,^[28] thereby strengthening the γ' phase.

The aim chemistry optimization phase for CMSX-4 alloy targeted maximization of creep-rupture response of the alloy using multistep 99%+ solution heat treatment procedures, and ensuring alloy microstructural stability. Extensive experience confirms that fully solutioned microstructures may be readily attained with CMSX-4 alloy airfoils in production vacuum heat treat furnaces with no incipient melting.

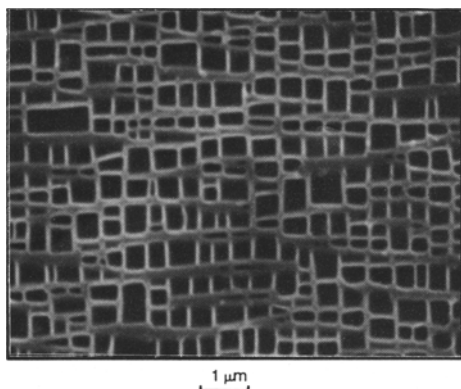


Fig. 2 Laboratory fully heat treated airfoil γ' microstructure (SEM) of CMSX-4 alloy (V 8154) second stage solid blade SX cast by Allison.^[25] CM 99% + solution. AC + 6 h/2085 °F (1140 °C), AC + 20 h/1600 °F (871 °C) AC. LE airfoil upper, longitudinal.

1.1.2 Alloy Melting

The optimized vacuum induction refining (VIR) procedures developed for CMSX-2 and CMSX-3[®] alloys (discussed in Ref 11), were used to produce the seven CM V-3 furnace 8000-lb (3630-kg) heats of CMSX-4 alloy, melted to date. Table 3 shows the carbon, sulfur, nitrogen, and oxygen contents of these heats. Studies by several single-crystal (SX) casters demonstrate that high [N] and [O] levels in single-crystal superalloy ingot adversely affect single-crystal casting yield due to grain defects.^[30] The presence of [O], [N], and S master alloy impurities are known to transfer nonmetallic inclusions, such as aluminum oxide and nitrides and sulfides of tantalum and titanium, to SX parts.^[31]

The extensive development of the vacuum induction refining process for the CMSX-4 alloy ingot combined with clean single-crystal casting processes have resulted in both clean alloy and airfoil castings in terms of stable oxide dross or refractory inclusions. This is confirmed by the production of tens of thousands of single-crystal turbine blade castings ranging from 0.010 in. (0.25 mm) thick Lamilloy crystalfoils to large shrouded turbine blades for the new 80,000-lb thrust commercial turbofan engines, with attendant high process yields and low levels of grain defects.^[23]

1.1.3 Microstructure

Aging heat treatment studies have been undertaken, which show that the maximum creep strength throughout the 1500 to 2100 °F (816 to 1149 °C) testing range for (001) orientation specimens is attained with an average 0.45 μm cubic γ' aligned structure, with a 2085 °F (1140 °C) high-temperature aging treatment required. The relatively high aging temperature suggests that CMSX-4 has low γ/γ' misfit at high temperatures. A typical fully heat treated scanning electron micrograph (SEM) microstructure for a turbine airfoil is shown in Fig. 2. Solution treatment was undertaken in a laboratory tube furnace finishing at 2 h/2410 °F (1321 °C)/air cool (AC). This necessitates a 6 h/2085 °F (1140 °C)/AC age to achieve the desired γ' size. A final age of 20 h/1600 °F (871 °C)/AC is used. Commercial single-crystal turbine airfoils are vacuum solution treated using a

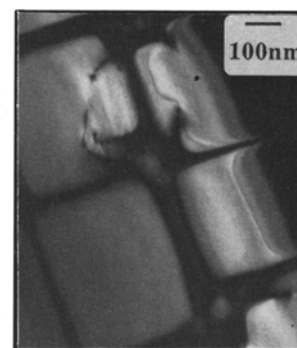
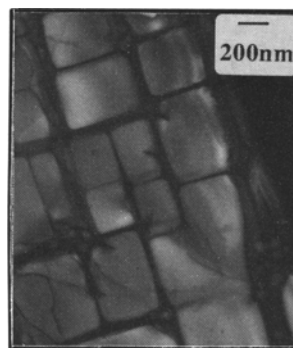


Fig. 3 (left) and **Fig. 4** (right) Laboratory fully heat treated CMSX-4 airfoil TEM microstructure.

Table 3 C, S, [N], and [O] content of CMSX-4 alloy V-3 furnace 100% virgin heats

Heat	Composition, wt ppm			
	C	S	[N]	[O]
V 7927.....	20	6	3	1
V 8053.....	19	5	2	1
V 8054.....	15	6	3	1
V 8154.....	21	3	2	2
V 8194.....	17	4	2	2
V 8195.....	18	4	2	2
V 8256.....	15	2	1	1

gas fan quench (GFQ) from the solutioning temperature, which only requires a several hour 2085 °F (1140 °C)/GFQ high-temperature age to achieve the required γ' structure.

Transmission electron microscope (TEM) foils from a laboratory fully heat treated CMSX-4 airfoil are shown in Fig. 3 and 4.^[32] Figure 3, in an ordering reflection, shows that the γ' varies in size locally and by a factor (linearly) of about 3. Also, the intervening γ has similar variations in thickness, with the formation of secondary, ultra-fine γ' in the broader γ gaps resulting from the final 1600 °F (871 °C) age. Energy-dispersive x-ray (EDX) composition profiles of the γ' and γ in the TEM foils show the expected trends, with the γ' being rich in (nickel, with some cobalt and chromium) and (aluminum, titanium, tantalum, and tungsten). The γ is rich in nickel, chromium, and cobalt—disproportionally larger for chromium relative to cobalt—as well as, of course, rhenium and tungsten. Recent research^[33] with TEM foils using an EDX-HP Ge detector and SRR 99 single-crystal alloy (Table 1) reveals that some steep element concentration gradients in the γ' phase persist even with an aged 0.5 μm cubic γ' microstructure. The enrichment of aluminum in the γ' at the γ/γ' interfaces is still significant, and the reduction of chromium at the interfaces is maintained. The average concentrations of elements in the γ' phase have not been changed significantly by the two-stage aging heat treatments. Interfacial γ/γ' chemistry is thought to be important in influencing creep response.

Research^[34] has shown that, for alloys with a high volume fraction of γ' (at a constant volume fraction), difficult-to-shear cuboidal γ' precipitates that are spaced as closely together as possible will provide optimum creep resistance. Any composi-

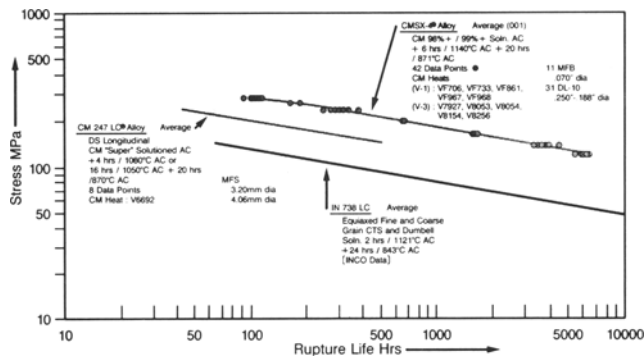


Fig. 5 Stress-rupture at 1800 °F (982 °C).

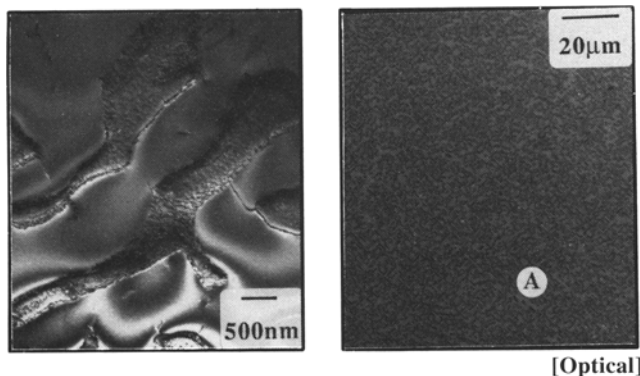


Fig. 6 (left) and Fig. 7 (right) CMSX-4 post-test TEM microstructure at 20 ksi/1800 °F (138 MPa/982 °C) after 3921 h_T .

tional adjustment that influences the level of misfit between the γ and γ' , the chemistry of the γ' , the equilibrium volume fraction of γ' , or its coarsening behavior will have significant effects on creep properties by changing the γ' morphology, shape, or the matrix gap dimension.

1.1.4 Creep-Rupture and Phase Stability

The stress-rupture temperature capability advantage of CMSX-4 alloy over CMSX-2/3 alloys is 64 °F (35 °C), based on density-corrected average properties, in the 36 ksi/1800 °F (248 MPa/982 °C) testing regime.^[23] The data also suggest that CMSX-4 alloy has useful strength at 2125 °F (1163 °C).^[23] The Larson-Miller stress-rupture database generated by CM includes over 250 data points from nine heats, including six 8000-lb (3630-kg) heats. These properties were undertaken on both 0.187-in. diam (4.8 mm) test bars and 0.070 in. diam (1.8 mm) machined-from-blade (MFB) specimens, with no fall-off in properties apparent with production heat scale-up to 8000 lb (3630 kg).

Industrial gas turbine applications for the alloy have necessitated creep-rupture testing out to 9000-h rupture life at 16.5 ksi/1800 °F (114 MPa/982 °C). The 1800 °F (982 °C) stress-rupture data shown in the log-stress to log-life plot in Fig. 5 reveal no fall-off in properties due to undesirable microstructural changes.

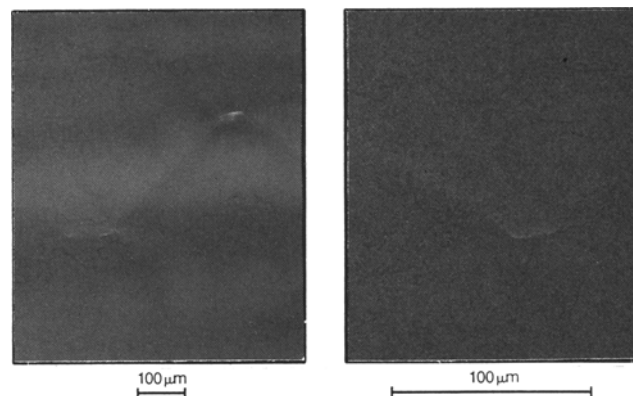


Fig. 8 (left) and Fig. 9 (right) CMSX-4 alloy (V 8054) SX test bar, 14 mm diameter, 99% + solution GFQ + IMT HIP, 15 ksi/2400 °F (1316 °C)/5 h, FC + CM resolution 3 h/2410 °F (1321 °C), AC. Longitudinal. (FC = furnace cool; AC = air cool.)

Microstructures of a post-test (0.25 in. diam, or 6.4 mm) specimen creep-rupture tested at 138 MPa/982 °C (20 ksi/1800 °F) for 3921 h_T , are shown in Fig. 6 and 7.^[32] The generally irregular format of the agglomerated γ/γ' structure is apparent. Extremely small (700 nm, or 0.7 μ m) rhombohedral topological intermetallic phases surrounded by γ' are barely discernible at point A in Fig. 7. Analytical TEM shows these phases to be ((Ni,Co)W)(Cr,Re) rich.^[32] However, no creep cracking has been found to be associated with these phases. It is postulated^[35] that the development of a range of extremely small heterogeneity in rhenium-containing single-crystal or DS superalloys during creep can be of fundamental importance to the improvement of creep behavior.

1.1.5 Mechanical Fatigue

The absence of significant residual γ/γ' eutectic phase, carbides, oxide, nitride, or sulfide inclusions and microporosity (resulting from the ability to readily fully solution CMSX-4 and HIP) (Fig. 8 and 9) results in remarkably high mechanical fatigue properties in smooth and particularly notched specimens. At 1382 °F (750 °C), the HCF strength of smooth specimens of CMSX-4 to 10^7 cycles N_f is improved 50% by HIP processing. The HIPing of CMSX-4 results in significantly greater mechanical fatigue property improvements compared to that obtained with non-rhenium containing alloys, indicating that the elimination of micropores is not the only important factor. Increased refractory element (tungsten, rhenium, and tantalum) homogeneity may also be relevant. Additionally, the superior creep strength of CMSX-4 alloy over first-generation single-crystal alloys is expected to be a significant advantage in HCF conditions where sufficient time is spent at stress and temperature to enable creep-fatigue interactions to occur.^[17]

1.1.6 Thermal Fatigue

The higher resistance of the oxide-scale in CMSX-4 to spalling combined with the higher strength of the corresponding γ' depleted zone improves its thermal fatigue crack initiation resistance in comparison with SRR 99 alloy (Table 1).^[37]

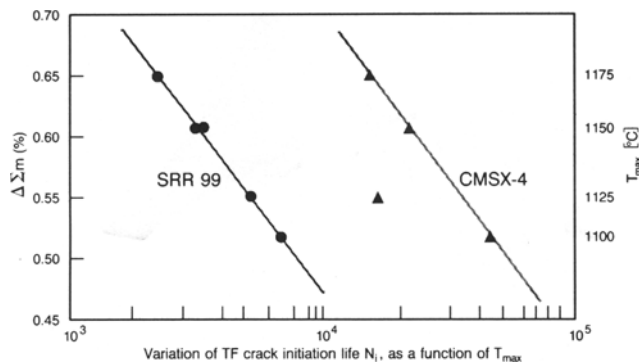


Fig. 10 TF crack initiation life, N_i

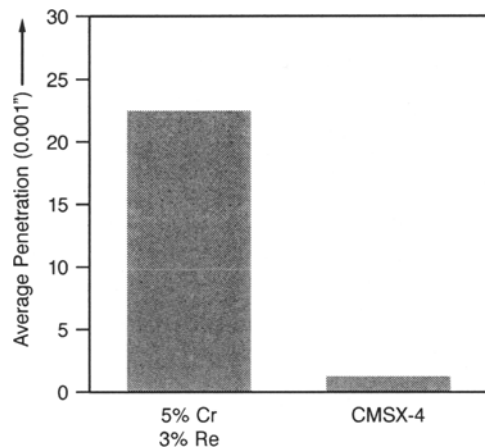


Fig. 11 Second-generation SX superalloy. Burner rig 1650 °F (899 °C); hot corrosion (uncoated) [1% sulfur, 10 ppm sea salt, 113 h test]

See Fig. 10. In CMSX-4, cracks initiate from small pores, whereas in SRR 99 crater-like regions are formed by a mechanism of successive oxide-scale spalling and re-oxidation of the base metal during thermal fatigue.

1.1.7 Oxidation and Hot Corrosion

Cyclic burner rig testing has shown CMSX-4 to have excellent high-temperature bare oxidation resistance.^[23] Burner rig sulfidation testing under a variety of type I hot corrosion test conditions (e.g., Fig. 11) shows the alloy to have performance similar to IN 792 in longer term testing.

1.1.8 Industrial Gas Turbine Experience

CMSX-4 alloy was introduced for turbine blading in the Solar Turbines Inc. Mars T-14000 engine in 1990. This resulted from the need for increased durability in the updated Mars engine. The initial engine field test was performed at a natural gas pipeline station where the engine was used to drive a Solar C-601 gas compressor set. In this engine, the first stage turbine rotor (Fig. 12) had a "rainbow" set of blades with test variables that included blade alloy (CMSX-4 and equiaxed MAR M 247) coatings, cooling flow, and minor blade geometrical differ-

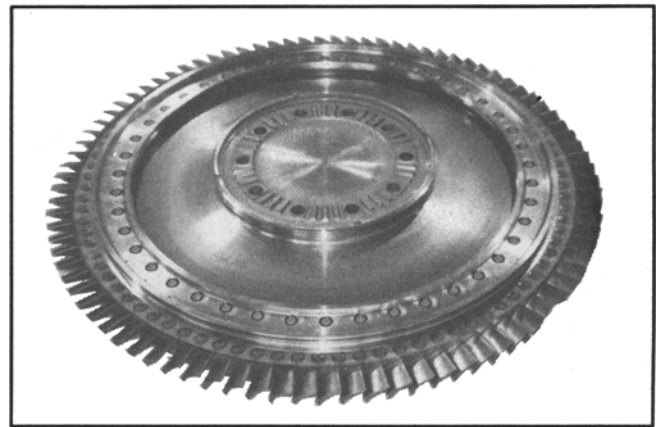


Fig. 12 Solar Mars T-14000 first stage turbine assembly. CMSX-4 blades.

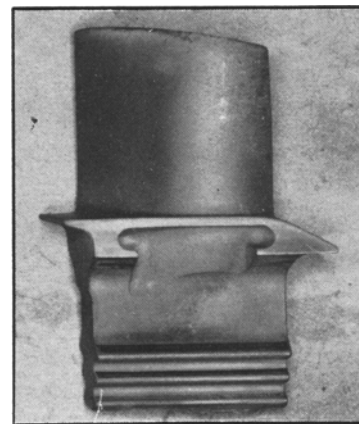


Fig. 13 Solar Mars T-14000 first blade in CMSX-4 after 4333 service hours.

ences. The engine was removed for inspection after accumulating 4333 service hours and 44 starts. The engine was fueled on natural gas.

During teardown inspection, it was observed the blades were in good condition. Typical as-received and after-test blades are shown in Fig. 1 and 13. Representative components were removed for detailed metallurgical evaluation and replaced with new parts. The remaining hot section components were replaced in the engine with the plan to continue the engine test for a total of 20,000 h. At the time of writing, they have accumulated an additional 8000 h in the engine at full-rated conditions.

Metallographic sections of removed blades were prepared at the tip and 70% span locations to determine their condition after 4333 h of engine operation. The results may be summarized as follows.

As shown by radial sections, blade tip integrity was better for the CMSX-4 blades in both coated and uncoated conditions compared to the standard MAR M 247 blades.* As anticipated, none of the platinum aluminide coated blades showed any significant oxidation. For uncoated blades, maximum depth of oxidation was greater for the MAR M 247 compared to the

Table 4 CM 186 LC alloy

C	Cr	Co	Mo	W	Nominal composition, wt%								Density, kg/dm ³
					Ta	Re	Al	Ti	B	Zr	Hf	Ni	
0.07	6	9	0.5	8	3	3	5.7	0.7	0.015	0.005	1.4	bal	8.70

Table 5 CM 186 LC alloy V-3 furnace 8000 lb (3630 kg) 100% virgin heat

Heat	C, wt%	Composition		
		S, ppm	[N], ppm	[O], ppm
V 8127.....	0.069	4	1	1

CMSX-4 blades and was related to the more rapid attack along grain boundaries and MC carbides. Interdiffusion of coating and substrate occurred to a lesser extent with the CMSX-4 blades.

Coarsening of the γ' and rafting was observed in the CMSX-4 SX blades at locations corresponding to extreme high temperatures and in MAR M 247 blades at locations corresponding to lower temperatures in the 1700 °F (927 °C) range and above.

Acicular phases were formed at the coating/substrate interface (diffusion zone) in both MAR M 247 and CMSX-4 alloys. In general, the incidence of these phases was greater in the MAR M 247 and occurred at lower temperature locations in the blades. For example, acicular phases were observed at the 70% span locations of the MAR M 247 blades, whereas at the same locations of the SX blades, roughly spherical particles of a Re/Cr/W-rich phase were present at the coating/substrate interface.

A very small amount of acicular phase formation occurred within the bulk sections of the CMSX-4 blades in the dendrite central regions. In this context, it should be noted that the original heat treat schedule comprising the lower temperature primary age (1975 °F, or 1080 °C versus 2085 °F, or 1140 °C) was used for the SX parts.

CMSX-4 is currently bill-of-material in production versions of the Mars T-14000 engine, with an estimated 80,000 total hours of successful accumulated running time.

1.2 CM 186 LC Superalloy

Vane component design is tending toward more complex cooling configurations with thin walls (0.020 in., or 0.5 mm) to improve engine efficiency through reduced use of cooling air. These complex vane segments can be difficult and expensive to manufacture as single crystals. CM 186 LC alloy, a second-generation DS columnar grain superalloy, has been developed with both component producibility and economic objectives in mind. The nominal composition and some of the critical tramp element chemistry of the first 8000-lb (3630-kg) CM V-3 furnace heat of the alloy is shown in Tables 4 and 5. The chemistry concepts for excellent DS castability were developed for CM 247 LC[®] alloy^[13] and further refined for the higher strength rhenium-containing alloy. Its DS castability, in terms of free-

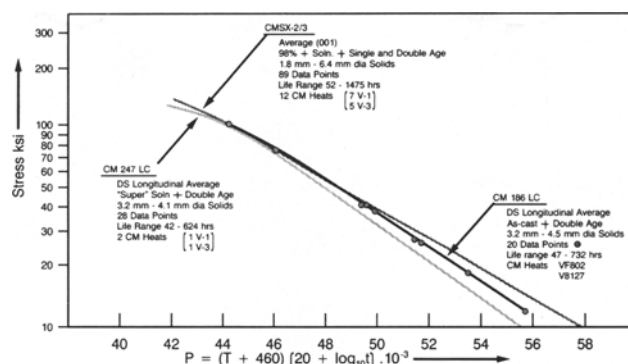


Fig. 14 Larson-Miller stress-rupture DS longitudinal CM 186 LC versus CM 247 LC versus CMSX-2/3 (001).

dom from DS grain boundary cracking, is excellent, particularly in casting advanced first stage vanes for a new turbofan engine, where cracking and tearing problems are encountered with a lower strength, established first-generation DS alloy. CM 186 LC alloy is used in the as-cast and double aged condition, which confers DS longitudinal creep-rupture properties equivalent to first-generation single-crystal alloys CMSX-2 and CMSX-3 up to 1800 °F (982 °C). Strength at higher temperatures lies between CMSX-2/3 and the solution treated DS alloy CM 247 LC (Fig. 14). The absence of a solution treatment requirement with CM 186 LC DS vanes eliminates the recrystallization problem and reduces process costs. The family derivation ensures that CM 186 LC alloy can be manufactured from virgin/CMSX-2, -3, or -4 foundry revert blends, further improving economics of manufacture.

DS transverse stress-rupture ductility of CM 186 LC in the ductility trough region at 55 ksi/1600 °F (379 MPa/871 °C) is typically 9% elongation in 4D. Satisfactory phase stability has been demonstrated up to 3500 h rupture life at 21.76 ksi/1742 °F (150 MPa/950 °C) and 400 h rupture life at 12 ksi/2000 °F (83 MPa/1093 °C).

CM 186 LC alloy has been successfully scaled to a 8000-lb (3630-kg) production-size heat, and the performance of a 50% virgin/50% CMSX-4 foundry revert heat has been validated. Oxidation, type I hot corrosion (sulfidation), and coating performance has been demonstrated on cyclic burner rig testing to be superior or similar to MAR M 247 alloy.

2. Conclusions

Turbine blade engine test evaluation by Solar Turbines Inc. confirms the overall properties of CMSX-4 alloy exhibited during the laboratory evaluation testing. The beneficial role of rhenium in contributing to the overall properties of the alloy are clearly apparent. CM 186 LC alloy has demonstrated DS vane

* MAR M is a trademark of Martin Marietta Corporation.

producibility and overall mechanical and environmental property results to justify turbine engine test evaluation scheduled to commence in late 1993.

References

1. M. Gell, D.N. Duhl, and A.F. Giamei, 4th Int. Symp. Superalloys, Seven Springs, PA, TMS Proceedings, Sept 1980, p 205-214
2. C.S. Wukusick, Final Report NAVAIR Contr., N62269-78-C-0315, 25 Aug 1980
3. J.W. Holmes et al., ASTM STP 942, 1988, p 672-691
4. T.E. Strangmen et al., 4th Int. Symp. Superalloys, Seven Springs, PA, TMS Proceedings, Sept 1980, p 215-224
5. M.J. Goulette, P.D. Spilling, and R.P. Arthey, 5th Int. Symp. Superalloys, Seven Springs, PA, TMS Proceedings, Oct 1984, p 167-176
7. M. Doner and J.A. Heckler, Aerospace Tech. Conf., Long Beach, CA, Oct 1985
6. D.A. Ford and R.P. Arthey, 5th Int. Symp. Superalloys, Seven Springs, PA, TMS Proceedings, Oct. 1984, p 115-124
8. E. Bachelet and G. Lamanthe, Nat. Symp. SX Superalloys, Viallard-de-Lans, France, 26-28 Feb 1986
9. M. Yamazaki et al., 5th Int. Symp. Superalloys, Seven Springs, PA, TMS Proceedings, Oct 1984, p 157-166
10. D.A. Petrov and A.T. Tumanov, *Aircraft Eng.*, No. 9, 1973
11. K. Harris, G.L. Erickson, and R.E. Schwer, ASME Paper No. 83-GT-244
12. K. Harris, G.L. Erickson, and R.E. Schwer, TMS Meeting, 3 Oct 1983
13. K. Harris, G.L. Erickson, and R.E. Schwer, 5th Int. Symp. Superalloys, Seven Springs, PA, TMS Proceedings, Oct 1984, p 221-230
14. K. Harris, G.L. Erickson, and R.E. Schwer, Cost 50/501 Conf., Liège, 6-9 Oct 1986, p 709-728
15. J. Wortmann, R. Wege, K. Harris, G.L. Erickson, and R.E. Schwer, 7th World Conf. Inv. Casting, Munich, 29 June 1988
16. N. Yukawa et al., 6th Int. Symp. Superalloys, Seven Springs, PA, TMS Proceedings, Sept 1988, p 225-234
17. A.D. Cetel and D.N. Duhl, 6th Int. Symp. Superalloys, Seven Springs, PA, TMS Proceedings, Sept 1988, p 235-244
18. M. Gell, D.N. Duhl, D.K. Gupta, and K.D. Sheffler, *JOM*, July 1987, p 11-15
19. T. Khan and M. Brun, Symp. SX Alloys, MTU/SMCT, Munich, June 1989
20. S.H. Ai, V. Lupine, and M. Maldini, *Scr. Metall. Mater.*, Vol 26, 1992, p 579-584
21. V. Lupine, Symp. SX Alloys, MTU/SMCT, Munich, June 1989
22. A.D. Cetel, B.A. Cowles, D.N. Duhl, D.P. DeLuca and M.L. Gell, *NASA Tech. Briefs*, Nov 1991, p 62, 63
23. K. Harris, G.L. Erickson, R.E. Schwer, D.J. Frasier, and J.R. Whetstone, Proc. Cost Conf. Liège, 24-27 Sept 1990, Part II, p 1281-1300
24. T. Khan, Symp. SX Alloys, MTU/SMCT, Munich, June 1989
25. *Aviation Week Space Technol.*, 24 Feb 1992, p 130-131
26. A.F. Giamei and D.L. Anton, *Metall. Trans. A*, Vol 16, 1985, p 1997
27. D. Blavette, P. Caron, and T. Khan, *Scr. Metall.*, Vol 20 (No. 10), Oct 1986
28. R. Darolia, D.F. Lahrman, and R.D. Field, 6th Int. Symp. Superalloys, Seven Springs, PA, TMS Proceedings, Sept 1988, p 262
29. D. Blavette, P. Caron, and T. Khan, 6th Int. Symp. Superalloys, Seven Springs, PA, TMS Proceedings, Sept 1988, p 305-314
30. D.C. Pratt and D.H. Wilkinson, 6th World Conf. Inv. Casting, Washington DC, Oct 1984
31. S. Isobe et al. Proc. Int. Gas Turbine Conf., Tokyo, Oct 1983
32. S.B. Newcomb and W.M. Stobbs, SAM Report, 3 Apr 1992
33. R. Schmidt and M. Feller-Kniepmeier, *Metall. Trans. A*, Vol 23, Mar 1992, p 745-757
34. T.M. Pollock and A.S. Argon, 6th Int. Symp. Superalloys, Seven Springs, PA, TMS Proceedings, Sept 1988, p 285-294
35. S.B. Newcomb and W.M. Stobbs, SAM Report, Jan 1992
36. U.S. patent No. 4,935,072 (Garrett-Allied-Signal Propulsion Engine)
37. F. Meyer-Olbersleben, D. Goldschmidt, and F. Rezai-Aria, Seventh Int. Symp. Superalloys, Seven Springs, PA, TMS Proceedings, Sept 1992, p 785-794